IET Research Journals
IET Journals The Institution of Engineering and Technology

A low-cost mechanism to reconfigure the operating frequency band of a Vivaldi antenna for cognitive radio and spectrum monitoring applications

ISSN 1751-8644
doi: 0000000000
www.ietdl.org

Cristina Borda-Fortuny[1,2] *Kin-Fai Tong*[1] *Kevin Chetty*[2]
[1] *Department of Electronic and Electrical Engineering, University College London, London, UK*
[2] *Department of Security and Crime Science, University College London, London, UK*
* *E-mail: k.tong@ucl.ac.uk*

Abstract: A frequency agile Vivaldi antenna whose operating frequency band can be switched between two selected bands is proposed in this paper for spectrum monitoring and cognitive radio applications. A RF switch is introduced into the back-slot of a Vivaldi antenna to allow switching of the operational band. The realised gains of the antenna are 10.5 dBi in the low band around 3.1 GHz, and 12 dBi in high band around 4.1 GHz. The radiation pattern is stable and its direction is consistent across the two bands. This design can be applied to multiple reconfigurable bands by using more RF switches to tune the desired operating frequency. A set of reliable design equations has been provided as well. This reconfigurable antenna offers improved gain and isolation over multiple, wideband and multiband antennas without increasing the cost and size when compared to those designs reported.

1 Introduction

Spectrum monitoring applications require antennas with wide bandwidth characteristic [1]. Multi-resonant antennas are not suitable because they operate in different modes and produce different radiation patterns, thus, the main lobe may not point at the desirable direction when tuning the band.

Wideband spectrum sensing is critical for efficiently finding spectral opportunities in cognitive radio as well [2]. Therefore, a wideband antenna that maintains a constant radiation pattern across its bands is required [3].

Not many antennas can achieve very wideband operation while maintaining high gain, high isolation between bands and a consistent radiation pattern. Several antennas have been proposed in [4–6] but they sacrifice the gain for tuning the operating frequency. Other existing designs suffer from variations in the radiation pattern, particularly the direction of the main lobe [7]. High isolation between frequency bands is also required to reject signals from adjacent bands therefore achieving higher SNR and jamming resistance [8]. Although some antennas have been reported for wideband tuning and high gain, they do not provide high rejection for close bands [9–11]. And other designs providing isolation, but they compromise the high gain as reported in [12–17].

To date, the reports of such antennas that can meet all the requirements for spectrum monitoring and cognitive radio in the literature are rare, therefore, a novel design is needed. In this paper a simple and effective wideband frequency reconfigurable antenna with consistent radiation pattern, high gain and high isolation is proposed. A Vivaldi antenna is utilized as the base for the proposed reconfigurable antenna because of its consistent radiation characteristics in its whole wide frequency band [18].

To avoid the gain deterioration, this paper proposes a microstrip line fed reconfigurable Vivaldi antenna which is optimized for the frequencies of interest and can reject the undesirable frequency bands. By controlling the resonant length of the back-slot of the Vivaldi antenna by the mean of a RF switch and the length of the open-circuited stub of the microstrip feed line, the undesirable frequency band can be rejected while a preferred band can be selected. As the RF switch determines the length of the signal path for the operating frequency band, therefore the desirable high frequency band can be simply adjusted by selecting the proper location of the RF switch based on the design equations provided in Section 3.

2 Antenna Geometry and Design

The proposed antenna is designed on a single microwave substrate as shown in Fig. 1. The dielectric substrate used is Taconic RF-43 with ε_r=4.3 and thickness 0.762 mm. The top layer presents an open-circuited microstrip line. The stub-to-slot intersection is formed by a quarter guided wavelength ($\frac{\lambda_0}{4\sqrt{\varepsilon_{eff}}}$) microstrip stub and a three-quarter free-space wavelength ($\frac{3\lambda_0}{4}$) back-slot at the low frequency band. The intersection is highlighted in red in the Top Layer of Fig. 1. For maximum coupling, the stub length (L_{stub}) of the microstrip feedline should be a quarter wavelength or odd multiple of a quarter wavelength of the guided wavelength ($(2n+1)\lambda_g/4$ where $n \in \mathbb{N}$) and the back-slot length should be a quarter wavelength or odd multiple of three-quarter free space wavelength ($(2n+1)\lambda_0/4$ where $n \in \mathbb{N}$) at the operating frequency band. Any other operating frequency that does not meet either condition will be rejected. Three-quarter wavelength at the low frequency band is chosen for the back-slot, so enough space is available for tuning to a higher frequency band.

A RF switch is introduced on the back-slot to switch to high frequency band. The RF switch controls the signal path while setting maximum coupling in the stub-to-slot intersection to produce a higher operating band. To operate in the lower band (Switch is OFF), the switch enables the signal to use the full length of the back-slot. In the high band (Switch is ON), the length of the slot is shorter, therefore it only excites the desirable higher frequency band. Outside the operating frequency band, either the length of the open-circuited microstrip line or the back-slot is not optimum, therefore the signal is rejected. Particularly, when both conditions are not met, it provides high isolation.

To support the monitoring of those common wireless systems, a Vivaldi antenna is designed to operate from 1 GHz to 6 GHz

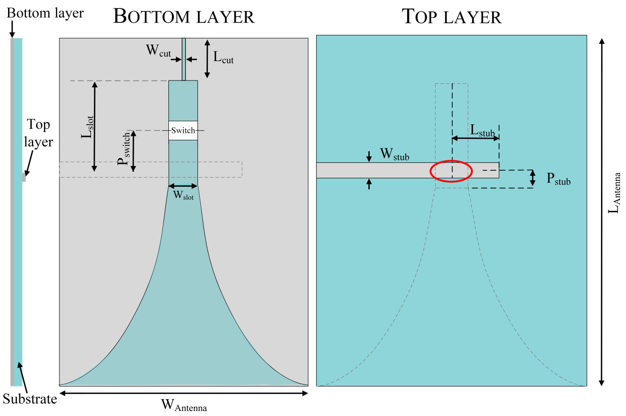

Fig. 1: Bottom layer (left) and top layer (right) of the two-band reconfigurable Vivaldi antenna geometry

following the equations in [19]. A low-insertion-loss RF switch (Hittite HMC550AE SPST [20]) is used as it provides adequate RF performances from DC to 6 GHz.

3 Technical Analysis

To support the research community, a set of reliable empirical equations is presented to calculate the antenna dimensions and switch position. The method also calculates the rejected frequencies with at least 14 dB isolation for each band with a minimum accuracy of 96.6% when compared to a commercial full-wave EM simulation. To extract these equations both transmission line theory and empirical experience are applied.

The design parameters equations for the passbands are presented in equations 1 – 4, in reference to those shown in Fig. 1. This method assumes a basic Vivaldi antenna is already designed and it covers the whole operating frequency bands of interest.

λ_{LB} represents the wavelength of the desired operating frequency in the low band and λ_{HB} represents the wavelength of the desired operating frequency in the high band. For the stub length (L_{stub}) and the stub position (P_{stub}) a trade-off is made between the two frequency bands by using the wavelength of the middle frequency between the low band and the high band, which is defined as $(\lambda_{LB} + \lambda_{HB})/2$.

$$Slot\ length\ (L_{slot}) = 0.8 \cdot \frac{3\lambda_{LB}}{4} \tag{1}$$

$$Stub\ length\ (L_{stub}) = 0.79 \cdot \frac{(\lambda_{LB} + \lambda_{HB})/2}{4\sqrt{\varepsilon_{eff}}} \tag{2}$$

$$Stub\ position\ (P_{stub}) = 0.76 \cdot \frac{(\lambda_{LB} + \lambda_{HB})/2}{4} \tag{3}$$

$$Switch\ position\ (P_{switch}) = 0.75 \cdot \frac{3\lambda_{HB}}{4} \tag{4}$$

Maximum transmission for the passband can be achieved when the slot length (L_{slot}) is about three-quarters of the free-space wavelength, the stub length (L_{stub}) is a quarter of the guided wavelength and the stub position (P_{stub}) is a quarter of the average free-space wavelength at the desired operating frequency bands. Based on the results from the intensive simulations, correction factors, between 0.75 to 0.8, is introduced in Eq. 1 to Eq. 4. to improve the accuracy of the equations.

A RF switch is introduced in the back-slot at the position calculated using equation 4 to evaluate the P_{switch} as presented in Fig. 1.

The wavelengths of the rejected frequencies ($\lambda_{rf1}, \lambda_{rf2}, \lambda_{rf3}, \lambda_{rf4}$) can be defined depending on the slot length (L_{slot}) and stub length (L_{stub}) for each design as well. When the slot length is equal to a half-wavelength (see Fig. 2a), a full-wavelength (see Fig. 2b) or multiples of these ($n\lambda_0/2$) (see Fig. 2c) for a particular frequency the resulting gain of the Vivaldi antenna in the direction of interest drops, as the signal is resonating in the slot. These are presented in equation 5 and equation 6. The stub length also determines rejected frequencies, as shown in equation 7 and equation 8. This occurs when the stub is a multiple of the half guided wavelength ($n\lambda_g/2$) (see Fig. 2d).

$$\lambda_{rf1} = 1.05 \cdot (2 \cdot L_{slot}) \tag{5}$$

$$\lambda_{rf2} = 1.15 \cdot L_{slot} \tag{6}$$

$$\lambda_{rf3} = 1.10 \cdot (2 \cdot L_{stub}) \tag{7}$$

$$\lambda_{rf4} = 1.11 \cdot L_{stub} \tag{8}$$

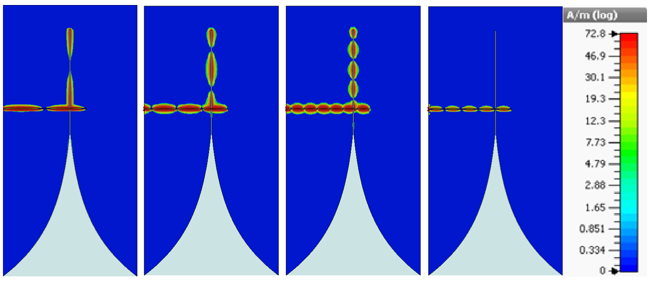

(a) (b) (c) (d)

Fig. 2: Current distributions for rejected frequencies in the reconfigurable Vivaldi antenna design when slot length is (a) half-wavelength, (b) one wavelength, (c) two wavelengths and (d) stub length is half-wavelength

Several models have been designed by using equations 1 – 8 and simulated using CST Microwave Studio [21]. The measured S-parameters of the RF switch are embedded in the simulation to obtain more accurate results in all the four bands. Fig. 3 presents the simulated results for 4 frequency bands: 2 GHz, 3 GHz, 4 GHz and 5 GHz. The antenna design parameters were first evaluated by using the 8 equations presented and then were further optimized by the commercial software. In the simulation of all the 4 frequency bands, the 2 GHz band showed the most deviation, therefore to keep the clarity of the figures, The 2 GHz band calculated by the formulas with no optimization, which is shown in dashed lines, is selected for comparison. The yellow arrow in Fig, 3b marks an isolation of 15 dB to the adjacent band with a difference of 0.3 dB between the 2 GHz band by formulas (in pink) and the 2 GHz band optimized (in red). When comparing the calculated results with the results from the commercial software, they presented a 96.6% accuracy calculated from the Relative Standard Deviation (RSD) for the design parameters presented in the equations as shown in Fig. 4. When evaluating the accuracy of one parameter, the other parameters were kept unchanged.

4 Two-band reconfigurable Vivaldi antenna

To further verify the accuracy of the design, a prototype based on equations 1 – 8 is fabricated. The design parameters and their values are indicated in Table 1.

For the switch to operate properly, a cut is required to separate the Vivaldi antenna in two halves for proper DC biasing of the switch. The width of the cut is 0.2 mm and the length is a quarter-wavelength

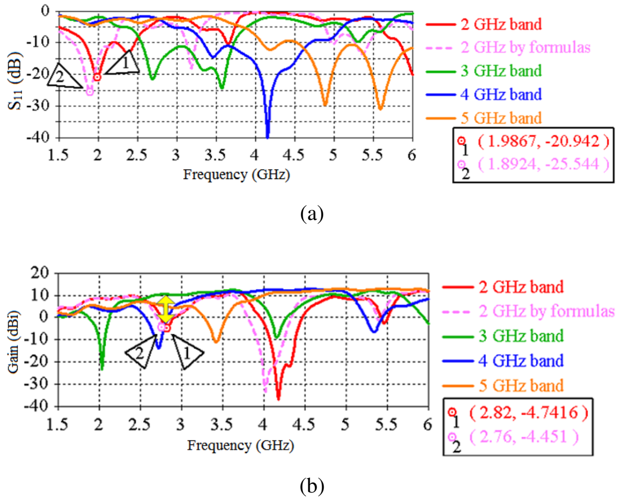

Fig. 3: Simulated (a) reflection coefficient and (b) realised gain for 4 frequency bands calculated using equations 1 – 8 and, then, optimized. As a comparison the 2 GHz band calculated using the formulas with no optimization (in pink dashed lines) is presented as well

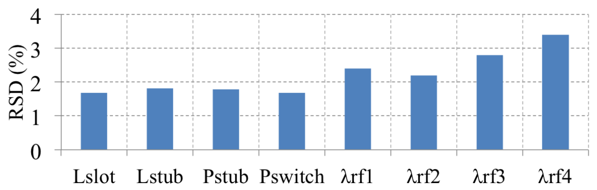

Fig. 4: Relative Standard Deviation calculated from the simulated results for the design parameters

Table 1 Design Parameters for the Two-Band Vivaldi Antenna

Parameter	Value (mm)	Parameter	Value (mm)
$L_{Antenna}$	250.0	$W_{Antenna}$	150.0
L_{slot}	60.0	W_{slot}	1.22
P_{switch}	40.0	L_{stub}	7.98
W_{stub}	1.5	P_{stub}	15.8
L_{cut}	20.0	W_{cut}	0.2

at the low frequency band, to transform an open circuit into a short circuit at the end of the back-slot.

Other switch requirements are: a control voltage between 0.0 V and 5.0 V, and a 100 pF DC blocking capacitor, which sets the lower cutoff frequency of RF switch to 1 GHz, connected to each RF port of the switch.

5 Analysis of surface current distributions

The current distributions are presented for the low and high frequency bands in Fig. 5. In-band operation occurs when the stub and slot are matched. The signal is propagated to the exponential flare of the antenna and radiated, as in Fig. 5a and Fig. 5d. The Vivaldi antenna is operating as a travelling-wave antenna and radiating. In out-band operation the signal is resonating and stays in the slot instead and, thus the antenna is not radiating as shown in Fig. 5b and Fig. 5c. In these cases, the stub and the back-slot are not matched causing the Vivaldi antenna to reject the undesirable band.

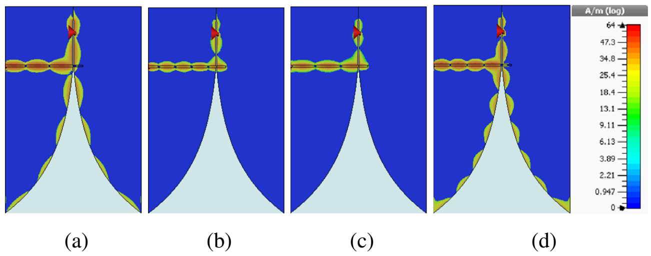

Fig. 5: Current distributions for a reconfigurable Vivaldi antenna design in (a) in-band low-band operation (at 3 GHz), (b) out-band low-band operation (at 4.2 GHz), (c) out-band high-band operation (at 3 GHz) and (d) in-band high-band operation (at 4.2 GHz)

6 Simulation and Measurement results

Fig. 6a shows the bottom layer with the exponential flare of the two-band reconfigurable Vivaldi antenna and Fig. 6b shows the top layer with the microstrip feed line and the soldered RF switch of the prototype.

The RF switch is soldered in the top layer but connected to the bottom layer through vias, as the usable space on the bottom layer is limited. This RF switch requires 2 pins connected to ground, 1 pin connected to Vdd, 1 pin connected to the controlling voltage and 2 pins connected to the RF signals to be switched. The footprint of the RF switch does not fit inside the back-slot of the bottom layer and would otherwise overlap and disturb the RF signals propagating in the back-slot. Thus, the RF switch is soldered in the top layer and the RF pins connected through vias to the bottom layer.

The small board on the top-left corner is connected to the RF switch in the top layer to switch the operating band of the antenna. It can be connected to a microcontroller that switches the bands automatically to suit cognitive radio applications, for example.

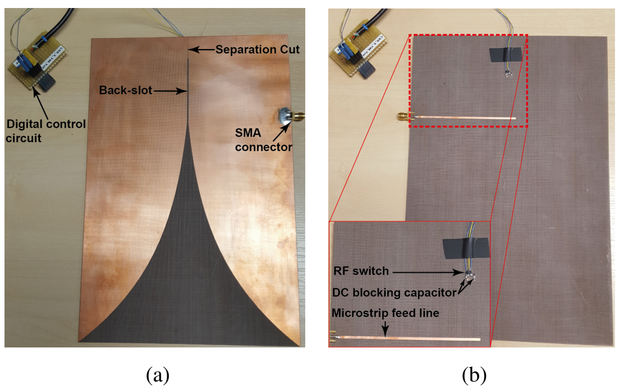

Fig. 6: (a) Bottom layer and (b) top layer of the prototype fabricated for the two-band reconfigurable Vivaldi antenna

Table 2 presents the specifications of a selection of the most significant antenna designs compared to the design proposed in this paper in terms of antenna requirements. "Bands" indicate the whole frequencies the antenna can operate at. To achieve a greater bandwidth most of the designs sacrifice the gain and isolation between bands [12, 13]. Although a Half-Vivaldi with a tunable stop band can achieve an isolation of up to 30 dB in some bands [10], the gain provided by the antenna is only 2 to 7 dBi, which makes it not suitable for high-band applications such as spectrum monitoring and cognitive radio. Most of the proposed designs present the gain with high fluctuations [9, 10, 13].

Fig. 7a shows a comparison between measured (solid lines) and simulated (dashed lines) reflection coefficient for the two-band reconfigurable Vivaldi antenna. The measured gain is compared to

This article has been accepted for publication in a future issue of this journal, but has not been fully edited.
Content may change prior to final publication in an issue of the journal. To cite the paper please use the doi provided on the Digital Library page.

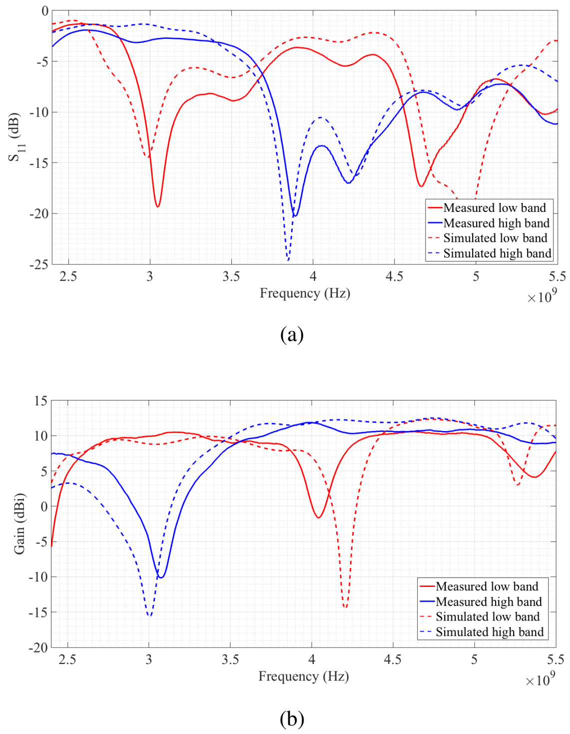

Fig. 7: Measured (solid lines) and simulated (dashed lines) (a) reflection coefficient and (b) gain for the two-band reconfigurable Vivaldi antenna

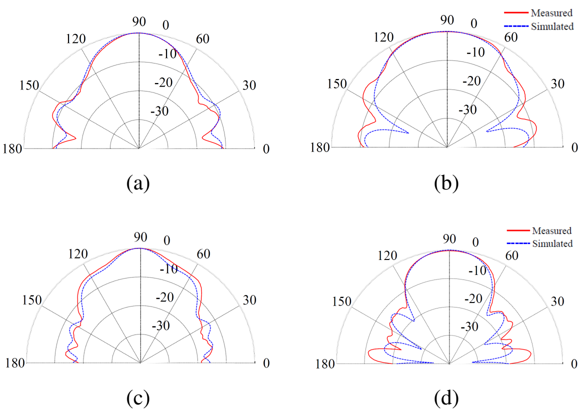

Fig. 8: Measured (red solid lines) and simulated (blue dashed lines) (a) E-plane, (b) H-plane radiation pattern for the low band and (c) E-plane, (d) H-plane for the high band

Table 2 Comparison with other Proposed Designs

Ref	Bands (GHz)	Gain (dBi)	Isolation (dB)
This work	1-6	10.5-12	15-20
[9]	2-7	1-6	13
[10]	2.3-6.7	2-7	18-30
[12]	2.2-11	Omnidirectional	< 7.5
[13]	3.3-10.6	2-5.5	<7.5

the simulated gain in Fig. 7b. Measured results are in good agreement with simulated results. The differences can be caused by the poor switch isolation between ON and OFF states, as the measured RF switch isolation between ON and OFF states is only 9 dB in the high frequency band. Table 3 summarises the results measured for the two bands.

Table 3 Measured Results for the Two-Band Vivaldi Antenna

Mode	*Centre frequency*	*Gain*	*Isolation*
Switch OFF	3.1 GHz (low band)	10.5 dBi	15 dB
Switch ON	4.1 GHz (high band)	12 dBi	20 dB

Fig. 8 compares the measured and simulated radiation patterns for the E-plane and the H-plane of the low band and the high band. In both frequency bands measured results agree with simulated results.

7 Conclusion

A two-band reconfigurable Vivaldi antenna that provides consistent radiation pattern, high gain and high isolation is proposed for spectrum monitoring and cognitive radio applications. The antenna can switch between two frequency bands by using a low-insertion-loss RF switch. A prototype of the proposed antenna is fabricated and verified in an anechoic chamber achieving good agreement with the simulation results.

8 References

1 C. G. Christodoulou, Y. Tawk, S. A. Lane, and S. R. Erwin, “Reconfigurable antennas for wireless and space applications,” *Proceedings of the IEEE*, vol. 100, pp. 2250–2261, July 2012.
2 H. Sun, A. Nallanathan, C. X. Wang, and Y. Chen, “Wideband spectrum sensing for cognitive radio networks: a survey,” *IEEE Wireless Communications*, vol. 20, pp. 74–81, April 2013.
3 M. I. Skolnik, “Introduction to radar,” *Radar Handbook*, p. 1990, 1962.
4 M. Hamid, P. Gardner, P. Hall, and F. Ghanem, “Review of reconfigurable Vivaldi antennas,” in *IEEE Antennas and Propagation Society International Symposium (APSURSI), 2010*, pp. 1–4, 2010.
5 M. Hamid, P. Gardner, P. Hall, and F. Ghanem, “Vivaldi antenna with integrated switchable band pass resonator,” *IEEE Transactions on Antennas and Propagation*, vol. 59, no. 11, pp. 4008–4015, 2011.
6 M. Hamid, P. Gardner, P. Hall, and F. Ghanem, “Reconfigurable Vivaldi antenna with tunable stop bands,” in *International Workshop on Antenna Technology (iWAT), 2011*, pp. 54–57, 2011.
7 D. M. Pozar, *Microwave engineering*. John Wiley & Sons, 2009.
8 J. Bernhard, *Reconfigurable Antennas*. Synthesis Lectures on Antennas and Propagation Series, Morgan & Claypool Publishers, 2007.
9 M. R. Hamid, P. Gardner, P. S. Hall, and F. Ghanem, “Reconfigurable vivaldi antenna with tunable stop bands,” in *2011 International Workshop on Antenna Technology (iWAT)*, pp. 54–57, March 2011.
10 X. Artiga, J. Perruisseau-Carrier, P. Pardo-Carrera, I. Llamas-Garro, and Z. Brito-Brito, “Design of vivaldi antennas with embedded reconfigurable stopband filter,” in *Proceedings of the 5th European Conference on Antennas and Propagation (EUCAP)*, pp. 2284–2288, April 2011.
11 N. Rezazadeh and L. Shafai, “A novel ultra-wideband pattern diversity antenna for high-gain applications,” in *2014 XXXIth URSI General Assembly and Scientific Symposium (URSI GASS)*, pp. 1–4, Aug 2014.
12 M. Bitchikh and F. Ghanem, “A three-resolution uwb frequency reconfigurable antipodal vivaldi antenna for cognitive radios,” in *The 8th European Conference on Antennas and Propagation (EuCAP 2014)*, pp. 3665–3668, April 2014.
13 M. Bitchikh and F. Ghanem, “Uwb to 30 narrow sub-bands frequency reconfigurable antipodal vivaldi antenna,” *Electronics Letters*, vol. 52, no. 19, pp. 1580–1582, 2016.
14 P. Bhartia and I. Bahl, “A frequency agile microstrip antenna,” in *Antennas and Propagation Society International Symposium, 1982*, vol. 20, pp. 304–307, 1982.
15 L. Liu and R. Langley, “Electrically small antenna tuning techniques,” in *Antennas Propagation Conference, 2009. LAPC 2009. Loughborough*, pp. 313–316, 2009.
16 J. Kiriazi, H. Ghali, H. Ragaie, and H. Haddara, “Reconfigurable dual-band dipole antenna on silicon using series mems switches,” in *IEEE Antennas and Propagation Society International Symposium, 2003.*, vol. 1, pp. 403–406 vol.1, June 2003.
17 S. I. Jafri, R. Saleem, M. F. Shafique, and A. K. Brown, “Compact reconfigurable multiple-input-multiple-output antenna for ultra wideband applications,” *IET Microwaves, Antennas Propagation*, vol. 10, no. 4, pp. 413–419, 2016.
18 P. J. Gibson, “The Vivaldi aerial,” in *9th European Microwave Conference, 1979.*, pp. 101–105, 1979.
19 A. A. H. Ameri, G. Kompa, and A. Bangert, “Study about tem horn size reduction for ultrawideband radar application,” in *2011 German Microwave Conference*, pp. 1–4, March 2011.
20 Hittite, “HMC550 datasheet,” December 2014. http://www.analog.com/media/en/technical-documentation/data-sheets/hmc550.pdf.
21 “CST Microwave Studio.” https://www.cst.com/Products/CSTMWS/.